The Sunyaev-Zel'dovich Effect: an Update

Mark Birkinshaw

Department of Physics, University of Bristol, Tyndall Avenue, Bristol BS8 1TL, U.K.

Abstract. Much progress has been made on observing the Sunyaev-Zel'dovich effect(s) in clusters of galaxies, and recent theoretical work has placed the interpretation of the new data on a more secure footing. The deductions that can be made about the baryonic mass fractions of clusters and the value of the Hubble constant are reaching interesting levels of accuracy. In the present article I review the data, theory, and deductions and make some suggestions about where substantial progress is needed over the next few years by pointing out some of the pitfalls in the use of the effect.

INTRODUCTION

The Sunyaev-Zel'dovich (SZ) effects arise from the scattering of microwave background photons by electrons in a hot gas. The magnitude of the dominant (thermal) effect depends on two factors:

1. The probability that a given microwave background photon is scattered as it passes through the gas. If this probability is low, then it is given by the optical depth,

$$\tau_{\mathrm{e}} = n_{\mathrm{e}}\, \sigma_{\mathrm{T}}\, L \tag{1}$$

   where n_{e} is the electron number density, σ_{T} is the Thompson scattering cross-section (appropriate for low-energy scatterings), and L is the path length through the scattering gas.

2. The shift in frequency of photons arising from the scatterings. If the electron gas is hotter than the photon gas then the photons gain energy, and the mean fractional frequency increase is the dimensionless electron temperature

$$\Theta_{\mathrm{e}} = \frac{k_{\mathrm{B}} T_{\mathrm{e}}}{m_{\mathrm{e}} c^2} \tag{2}$$

   where k_{B} is the Boltzmann constant, T_{e} is the electron temperature, m_{e} is the electron mass, and c is the speed of light.

The fractional change in specific intensity of the microwave background radiation as seen through the hot gas, compared with the intensity of the microwave background radiation seen away from the hot gas, is then a decrease in the low-frequency (Rayleigh-Jeans) part of the spectrum by an amount

$$\frac{\Delta I_\nu}{I_\nu} \approx -2\, \tau_{\mathrm{e}}\, \Theta_{\mathrm{e}} \tag{3}$$

where the factor -2 arises because of the slope of the spectrum in the Rayleigh-Jeans region (see Fig. 1). At higher frequencies the unusual nature of the spectrum of the SZ effect is revealed. In intensity terms it has a minimum near 128 GHz, a zero near 218 GHz, and a maximum near 370 GHz. This spectral signature is sufficiently strong that in maps of the sky the effect should be clearly distinguishable from primordial anisotropies in the microwave background, dust emission from our Galaxy and extragalactic sources, or active galactic nuclei.

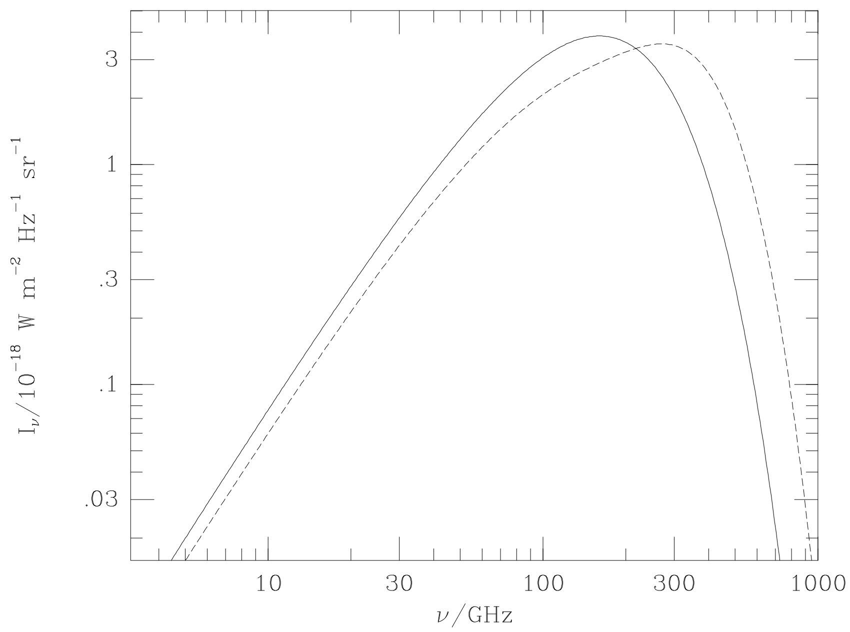

FIGURE 1. The spectrum of the microwave background radiation before (solid line) and after (dashed line) scattering by a hot gas with an exaggerated Comptonization parameter $y_C = \tau_e \Theta_e = 0.1$. The Sunyaev-Zel'dovich effect is the difference between these curves, and can be seen to be negative in the Rayleigh-Jeans region and positive in the Wien tail.

The thermal Sunyaev-Zel'dovich effect has a key property that makes it valuable for cosmology: an inspection of equation (3) shows that the SZ effect is redshift-independent, with ΔI_ν a function of the intrinsic properties of the hot gas through which the microwave background radiation is observed. This means that the SZ effect is a simple probe of free electron density structures in the Universe at all redshifts from $z = 0$ to recombination, provided that the electron overdensities and temperatures are sufficient to produce a detectable effect.

Generally only clusters of galaxies have dense enough atmospheres (τ_e up to a few times 10^{-2}) at high enough temperatures (Θ_e up to a few times 10^{-2}, corresponding to $k_B T_e$ up to 20 keV) for measurable effects (of a few times 10^{-4} in $\Delta I_\nu / I_\nu$). Thus the SZ effect is a measure of the properties of clusters of galaxies which hold substantial atmospheres.

These same clusters of galaxies are also luminous X-ray sources, and a comparison of the X-ray and SZ effect images of clusters provides information on the structures of the atmospheres. However the X-ray brightness of a cluster is *not* redshift-independent, and so at sufficiently large redshifts it might be expected that clusters would be more obvious through their SZ effects than their X-ray emission.

It should also be noted that the thermal SZ effect described above must also be accompanied by a second effect. If the scattering atmosphere responsible for the thermal SZ effect is moving relative to the Hubble flow, then a *kinematic* SZ effect must also be produced. This effect is proportional to the scattering probability and the peculiar radial velocity of the cluster

$$\frac{\Delta I_\nu}{I_\nu} = -\tau_e \frac{v_z}{c} \tag{4}$$

and has a spectrum like that of the microwave background radiation itself. This is sufficiently different from the spectrum of the thermal SZ effect that multifrequency observations of clusters of galaxies should be able to separate the thermal and kinematic effects, allowing the peculiar radial velocities of clusters to be measured. However, the kinematic effect is a factor $\sim 0.1 \left(v_z/1000 \text{ km s}^{-1}\right) \left(k_B T_e/10 \text{ keV}\right)^{-1}$ smaller than the thermal effect, and so will be difficult to measure. The best possibility of measuring it should be to measure the total SZ effect near 218 GHz, where the thermal effect has zero amplitude (Fig. 1).

Up to this point, I have summarized the "standard" properties of the SZ effects, which were already described by Sunyaev and Zel'dovich in their first paper on the effect [1]. Two substantial reviews of the observational and

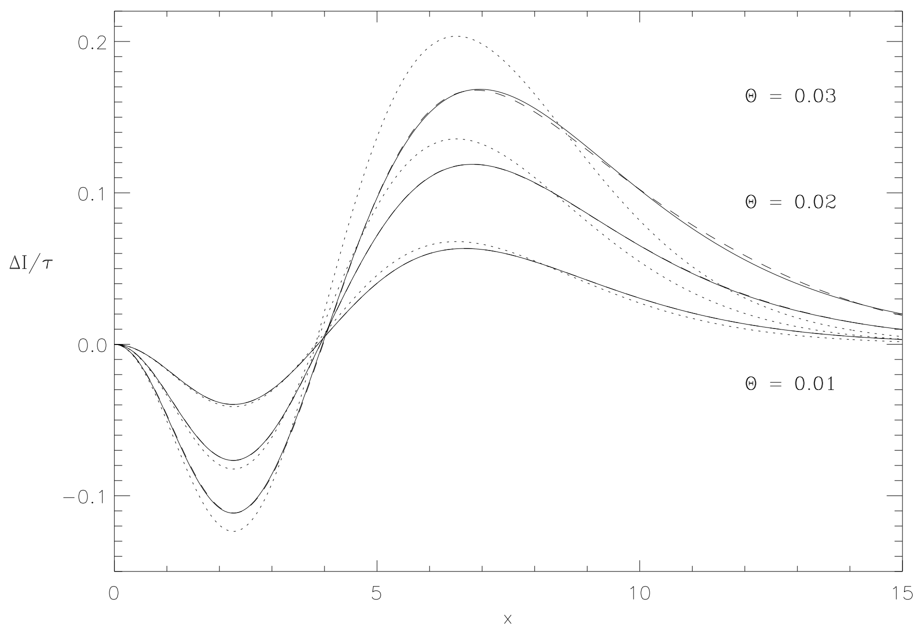

FIGURE 2. The spectrum of the Sunyaev-Zel'dovich effect as represented by the Kompaneets equation (dotted line), a correct relativistic treatment (solid line), and the fifth-order analytical approximation of Itoh et al. (long dashed line), for three dimensionless temperatures $\Theta_{\rm e} = 0.01$, 0.02, and 0.03 ($k_{\rm B} T_{\rm e} = 5$, 10, and 15 keV).

theoretical status of the effect have recently appeared [2,3], and in the remainder of this article I will provide glosses on these reviews' discussions of the effect, and warn of the pitfalls in using the effect uncritically

- to measure the Hubble constant;
- to measure the baryon fraction in clusters of galaxies;
- to measure cluster peculiar velocities; and
- to provide information on the evolution of clusters through a study of SZ effect confusion.

THEORETICAL UPDATE

Relativistic corrections

Until recently the spectrum of the SZ effect was always described by the equation

$$\Delta I(x) = I_0\, x^4\, y_{\rm C}\, \frac{e^x}{(e^x - 1)^2} \left(x \coth\left(\frac{x}{2}\right) - 4 \right) \tag{5}$$

which can be derived using the Kompaneets equation [4]. The Kompaneets equation simplifies the Boltzmann equation for the interactions of electrons and photons by treating only low-energy electrons and photons. In equation (5), $I_0 = \frac{2h}{c^2} \left(\frac{k_{\rm B} T_{\rm rad}}{h} \right)^3$ is the intensity scale of the microwave background radiation and $x = \frac{h\nu}{k_{\rm B} T_{\rm rad}}$ is a dimensionless measure of frequency. $T_{\rm rad} = 2.728 \pm 0.002$ K is the temperature of the microwave background radiation [5]. The strength of the interaction between photons and electrons is described by a single parameter, $y_{\rm C} \equiv \tau_{\rm e} \Theta_{\rm e}$, referred to as the Comptonization parameter.

Equation (5) is adequate if the scattering is non-relativistic. However, although the temperature of the scattering gas in most clusters is only ~ 5 keV, and hence $\Theta_{\rm e} \ll 1$, this implies that typical electron velocities may be as large as $0.1c$ and hence that the scattering is mildly relativistic. As a result, we might expect

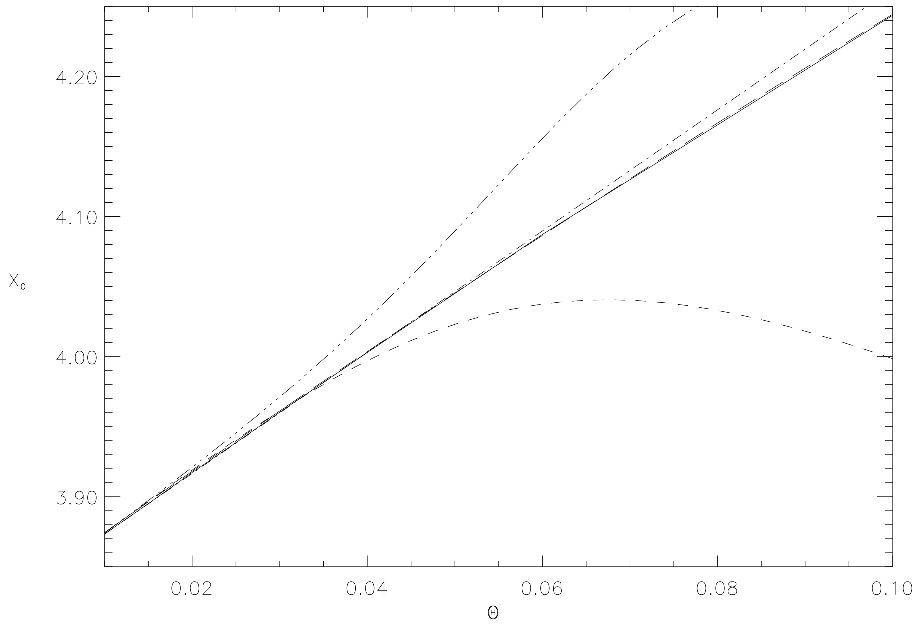

FIGURE 3. The dimensionless frequency of the zero of the thermal SZ effect, x_0, as a function of dimensionless scattering gas temperature, Θ_e, and calculated using a numerical integral of the Boltzmann equation (solid line) or a Monte-Carlo calculation (dashed line), a linear approximation (dash-dot line), and analytical approximations of third order (lower dashed line) or fifth order (dash three-dot line). The frequency of the zero is given by $\nu_0 = 56.8 x_0$ GHz. Figure from Molnar [9].

small variations of the spectrum from the form (5), with those variations becoming more significant as the temperature of the gas rises [6].

Over the past couple of years, several approximations for the spectrum of the SZ effect have appeared: these provide an equivalent to (5) for moderate or high gas temperatures. An indication of the change in spectral shape that is implied by the relativistic corrections is shown in Fig. 2. Fig. 2 also shows the fifth-order approximation to the spectral shape deduced by Itoh et al. [7] by examining perturbative solutions to the Boltzmann equation appropriate for mildly relativistic scatterings. Although the Itoh et al. approximation appears good, it has some difficulties at high frequencies ($x \gtrsim 6$, or $\nu \gtrsim 350$ GHz) where it becomes imprecise.

Beware these relativistic approximations! As emphasized by Challinor and Lasenby [8], the approximations are not guaranteed to be accurate because they are generated as asymptotic expansions of unreliable convergence properties. The problem is that the series approximation to the solution of the Boltzmann equation involves expansions in parameters which are not small, and hence the precision of the result is often low. This can be seen clearly in the different results for the location of the zero of the SZ effect as a function of Θ_e (Fig. 3). If this quantity is to be estimated, then Fig. 3 shows that the third and even fifth-order approximations of Itoh et al. [7] are less precise than the use of the simple linear approximation given by Birkinshaw [2] and Challinor and Lasenby [8].

Kinematic SZ effect

In a similar way there has been recent work on improving the approximations used in describing the kinematic SZ effect. Nozawa et al. [10] and Sazonov and Sunyaev [11] have taken account of terms of higher order in cluster peculiar velocity, and cross-terms of the type $\Theta_e \frac{v_z}{c}$, to produce more precise expressions than equation (4). These new results relax the usual assumptions [12] of zero gas temperature and highly non-relativistic cluster motion used to derive (4), but as expected the correction terms are generally small.

Beware the mistake of applying these corrections uncritically: they are generally used to express how the shape of the spectrum varies near the zero of the thermal effect, since it is through precise measurements of the

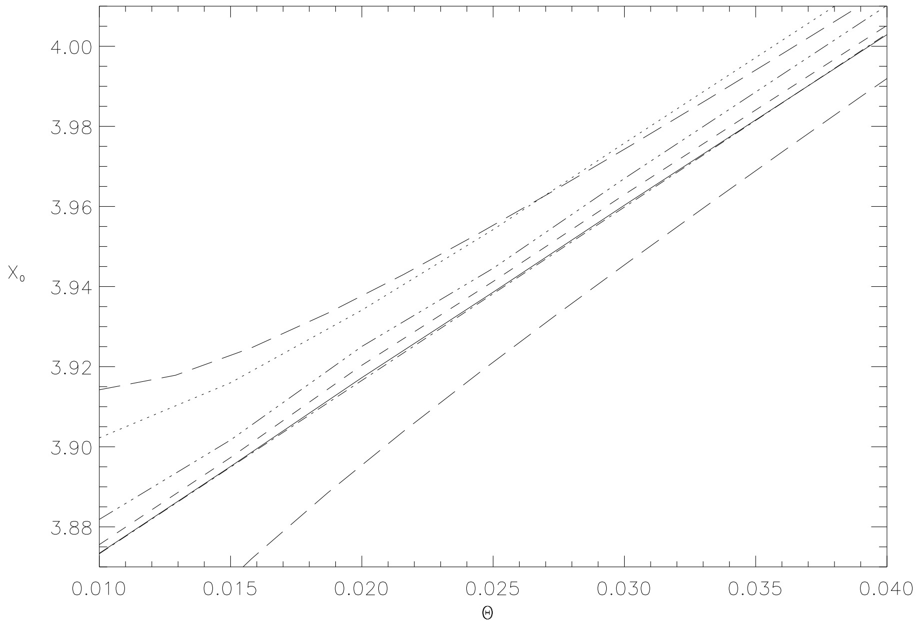

FIGURE 4. The dimensionless frequency of the zero of the combined (thermal plus kinematic) SZ effect, x_0, as a function of dimensionless scattering gas temperature, Θ_e, for different values of the optical depth τ_e (= 0, 0.02, 0.05, 0.1: solid, dashed, dash plus three dots, and dotted lines, respectively). Also shown is the effect of a ± 100 km s^{-1} cluster peculiar velocity (outer dashed lines). Variations of $1-2$ GHz in the frequency of the zero, $\nu_0 = 56.8 x_0$ GHz, arise from velocities of ~ 100 km s^{-1} and temperature changes of ~ 2 keV. From Molnar [9].

spectrum of the combined (thermal plus kinematic) SZ effect in this region that the cluster peculiar velocity can be measured. However, of critical importance in determining the shape of the spectrum of the combined SZ effect is the velocity distribution of the scattering electrons. Deviations from a thermal distribution or the presence of different temperature components within the cluster are likely to significantly change the spectrum of the SZ effect. It is also likely that the cluster gas is not precisely static, and its internal motions may confuse the shape of the spectrum. Optical depth effects in the gas, though small, are also important at the level of some of the cross terms.

The relative sizes of the kinematic and optical depth effects are illustrated in Fig. 4: it can be seen that the location of the zero of the combined thermal plus kinematic SZ effect is a relatively strong function of gas temperature and radial velocity. An error of 2 keV in the temperature of the gas corresponds to an error of 100 km s^{-1} in the velocity of the cluster.

A further limitation in the use of the kinematic SZ effect to measure the velocity of an individual cluster of galaxies is confusion with primordial fluctuations in the background radiation. The amplitude of this confusion depends on the angular size of the cluster and the power spectrum of primordial fluctuations: for clusters at redshifts ~ 0.1, an error of a few hundred km s^{-1} from this cause is inescapable. Of course, this implies that cluster peculiar velocities can be measured in an averaged sense, by comparing the distribution of apparent kinematic SZ effects on clusters with the same distribution at off-cluster positions: in the future this may be a valuable way of measuring the redshift evolution of the cluster velocity distribution, since the kinematic SZ effect, like the thermal SZ effect, is redshift-independent.

OBSERVATIONAL UPDATE

Radiometers

The first detections of the SZ effect were attempted with existing large single-dish telescopes, since these were available for the large tranches of observing time that were needed. The observations involved are exemplified

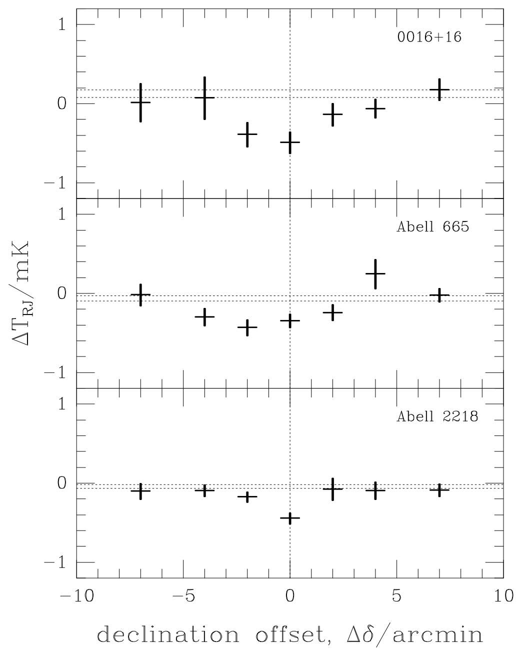

FIGURE 5. Measurements of differences in the apparent brightness temperature of the microwave background radiation as a function of declination near the centres of clusters CL 0016+16, Abell 665, and Abell 2218 (Birkinshaw et al. [14]). The largest SZ effect is seen near the centre of the cluster in each case, and the apparent locations of the centres and angular sizes of the effects are consistent with simple models based on the X-ray data.

by the early work of Birkinshaw et al. [13]. Although a number of detections were produced in this work (see Fig. 5), a variety of difficulties arise. Among these are

- strong atmospheric noise signals, which must be subtracted to high accuracy (using beam-switching and position-switching, or drift-scanning; see [2])
- confusion from background radio sources, which must be subtracted to moderate accuracy, which may be difficult if the sources are variable;
- ground pickup signals, which may be different in the two beams used in beam-switching and certainly vary in position-switching; and
- calibration errors (in relating the measured signal voltages to astronomical signals on the sky).

It is also necessary to be careful about the choice of telescope used to observe the SZ effects. For example, when observing with a dual-beam system on a large telescope, the two beams might each have full-width to half-maximum (FWHM) of 1.5 arcmin and be separated by 7 arcmin. In that case, clusters with SZ-effect FWHMs (which tend to exceed the X-ray FWHMs) of much more than 7 arcmin are subtracted out by the differencing between the "on" and "off" beam signals. Clusters with SZ effect FWHMs much less than 1.5 arcmin also appear fainter, in this case because of beam dilution. Hence for any telescope and observing strategy, there will be an optimum redshift band for which that telescope is most useful: for the case described here, that band is roughly for redshifts $0.1 - 0.5$ [2].

A large number of radiometer-derived SZ effects have now been reported: perhaps the most reliable are Abell 478, 665, 1656, 2142, 2218, and 2256 and CL 0016+16 [15,16,14]. This technique seems well-suited to making single-point (e.g., central) measurements of the SZ effects of a large sample of clusters: with modern equipment and a carefully-optimized telescope system, it is relatively efficient and simple, although careful checks for the presence of confusing non-thermal sources (e.g., by an associated programme of interferometric mapping) are essential.

Beware the uncritical use of reported measured SZ effects from radiometers. The effects of beam dilution and beam switching (or drift scanning, or other observing strategies) cause the measured signal to be only

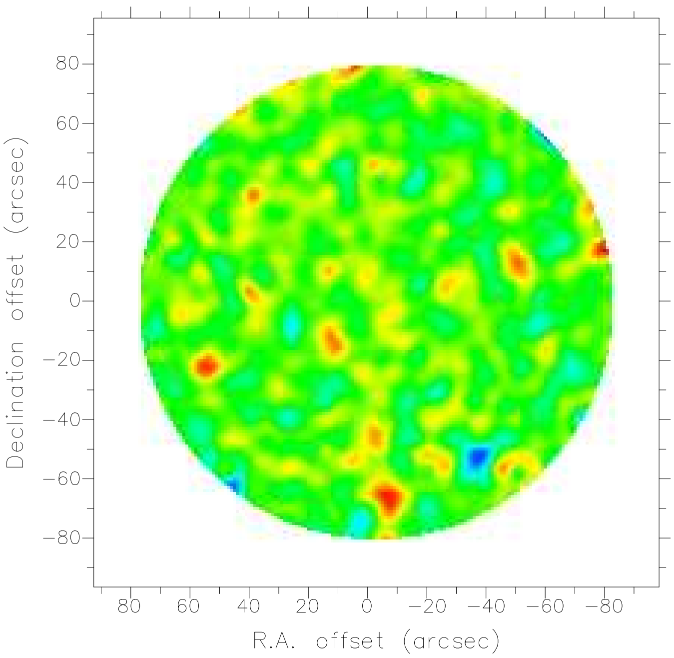

FIGURE 6. An image of cluster Abell 1689 at 850 μm, based on about four hours of integration with SCUBA on the JCMT. No strong SZ effect signal is visible in this representation of the data, since the noise level is still too high. However, an analysis of this noise field indicates a detection of the central SZ effect at the expected level for a Hubble constant near 50 $\mathrm{km\,s^{-1}\,Mpc^{-1}}$.

some fraction of the central SZ effect of the target cluster. Good knowledge of the beamshape of the telescope, the observing strategy, and the intrinsic shape of the cluster atmosphere is required to convert the measured signal into physical parameters for that atmosphere. Confusing radio sources, particularly variable sources, may also be a significant problem.

Bolometers

The principal advantage of a bolometric system over a radiometric system is the exceptional sensitivity that can be reached because of the very wide bandwidth that can be used. Furthermore, the best bolometer systems are now arrays, so that a small image of a cluster SZ effect should be generated in several bands simultaneously (e.g., using SCUBA on the JCMT). The principal disadvantage is that this bandwidth is obtained at a very high frequency (e.g., 350 GHz), where the atmosphere contributes an enormous signal. For this reason, bolometers are used on special-purpose mm-wave telescopes at high, dry sites (for example, at the CSO or the JCMT on Mauna Kea).

A major scientific reason for attempting to measure the SZ effect with a bolometric system is that at such high frequencies the data are sensitive to the spectrum of the SZ effect, and hence can be used to separate the thermal and kinematic effects. In good weather, we might expect a modern bolometer to detect a cluster SZ effect in a few hours, and to make a low signal/noise two-dimensional image of the cluster in a few days of integration.

An example of a bolometric image of a cluster for which a significant SZ effect is expected is shown in Fig. 6, which is based on about four hours of integration using SCUBA at 850 μm on the JCMT. No obvious SZ effect is seen on this image: the noise level (≈ 4 mJy) is such that the central SZ effect should be detected as a positive signal at a signal/noise of about one. At the edge of the array the signal/noise is significantly lower, but a slight positive signal is still expected. When the data are radially averaged, the central SZ effect can be fitted as 3.5 ± 1.6 mJy at 850 μm. This is consistent with the measurement of the central SZ effect by Holzapfel et al. [17], made with SuZIE on the CSO. Of interest in the image of Fig. 6 is the presence of a few significant emission peaks, which appear to be a confusing population of sub-mm sources, perhaps enhanced in brightness by the lensing effect of this massive cluster [18].

An illustration of the usefulness of bolometers in measuring the mm to sub-mm wave spectrum of a cluster of galaxies is provided by the composite spectrum of Abell 2163 measured by IRAS, ISO, PRONAOS, SuZIE, and Diabolo (Lamarre et al. [19]). The overall spectrum is best fitted by a composite model including the thermal (and possibly kinematic) SZ effects and dust emission. A warning for future bolometric observations is implicit in this result: with measurements at only a few (e.g., three) passbands, it would not be possible to infer the amplitude of the thermal or kinematic SZ effect without assumptions about the amplitude of the dust signal. Even at wavelengths as long as 1 mm, the dust signal makes a noticeable contribution to the SZ effect. Furthermore, as seen in Fig. 6, high angular-resolution observations of the cluster might be needed to check that some of the measured signal is not coming from confusing background (or foreground) sources.

Beware the uncritical use of reported measured SZ effects from bolometers. Just as for radiometers, the effects of beam dilution and the observing strategy cause the measured signal to be only some fraction of the central SZ effect of the target cluster (often less than half). Once again, a good knowledge of the beamshape of the telescope, the observing strategy, and the intrinsic shape of the cluster atmosphere is required to convert the measured signal into physical parameters for that atmosphere. At typical bolometer frequencies, the confusing effects of foreground dust and of dusty galaxies are potential problems.

Interferometers

The major success story of SZ effect observing in the past few years is the mapping of the effects using small cm-wave interferometers (sometimes mm-wave interferometers equipped with cm-wave receivers). The power of this technique is that it generates detailed images of SZ effects, which are valuable for making comparisons with X-ray images, while avoiding some of the systematic difficulties of the other techniques. Interferometry is probably the most rapidly-growing area for observation of SZ effects, and several new instruments for doing this work are currently under development.

The extra angular resolution that is available using interferometers is also a handicap. Interferometers work by measuring some range of Fourier components of the radio brightness distribution on the sky, and then recover an image of the sky brightness distribution by a back Fourier transform of the data, correction for the polar diagram functions of the individual antennas, and removal of the sampling function due to the antennas' sparse distribution on the ground. Since the Fourier components are measured by correlating the signals of pairs of antennas, and there is always some gap between those antennas, the use of an interferometer results in the loss of information about the structure of a source on large angular scales (we say that the large-scale structure is "resolved out" by the interferometer). Since the SZ effects of clusters of galaxies have angular sizes of several arcminutes in all cases, most interferometers will resolve out a significant fraction of the SZ effect. Even interferometers which have successfully mapped the SZ effects of clusters still lose a significant fraction of the signal (e.g., the Ryle telescope and the Owens Valley Millimeter Array [20,21]).

Much observing time with interferometers has been dedicated to the SZ effect recently, and as a result a large number of clusters have been detected and mapped, some by several arrays. A good example is the cluster CL 0016+16 at redshift 0.55, where interferometric measurements of the SZ effect have been reported by [21,22]) and are consistent with earlier radiometric measurements [14].

Beware, nevertheless, the uncritical use of reported measured SZ effects from interferometers. Just as for radiometers and bolometers, the configuration of observing system (in this case, the size of the antennas and their separations) can cause the measured signal to be only a small fraction of the central SZ effect of the target cluster (often much less than half). Once again, a good knowledge of the beamshape of the telescope, the observing strategy, and the intrinsic shape of the cluster atmosphere is required to convert the measured signal into physical parameters for that atmosphere. This must also be remembered in looking at images of the cluster SZ effects: only structure on a narrow range of angular scales is usually represented.

RESULTS

A recent catalogue of SZ effect measurements has been given in [2], and will not be attempted here: rather I will discuss some of the recent uses of the SZ effect data and the current problems. I have not attempted to be exhaustive, for example I will say nothing about the comparison of the SZ effect and X-ray images of clusters

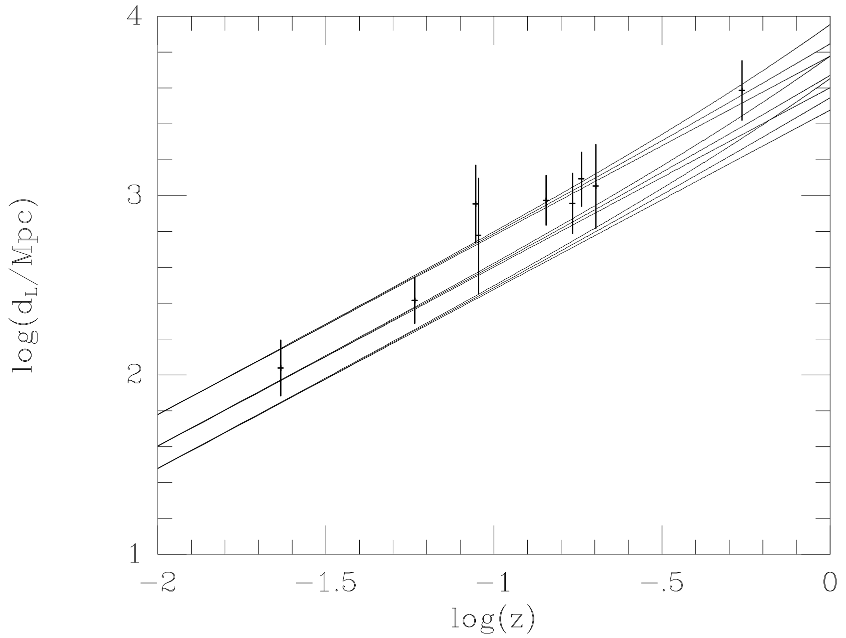

FIGURE 7. The Hubble diagram based on distances for nine clusters of galaxies, and with relativistic corrections. Measurements of the luminosity distance, $d_{\rm L}$, are shown for each cluster, and curves of $d_{\rm L}(z)$ are shown for $H_0 = 50$, 75, and 100 $\rm km\,s^{-1}\,Mpc^{-1}$ with $q_0 = 0$, $\frac{1}{2}$, and 1.

to study their atmospheres, but rather I highlight some uses which have been particularly heavily discussed in the literature or which seem to me to be specially interesting.

Hubble constant

When a cluster is imaged in X-rays and the thermal SZ effect we obtain information about the cluster's projected shape, the intensity scale of the X-ray surface brightness in some energy bandpass, $b_{\rm X} \propto \langle n_{\rm e}^2 \rangle L$, and the intensity scale of the SZ effect, $\Delta I_\nu \propto \langle n_{\rm e} \rangle L$, where the averages are taken along a particular fiducial line of sight and L is a measure of the depth of the cluster along that line of sight. The measured quantities $b_{\rm X}$ and ΔI_ν can be combined to provide an estimate of L,

$$L \propto \frac{\Delta I_\nu^2}{b_{\rm X}} \tag{6}$$

and then a comparison of L with the angular size of the cluster (from the X-ray or SZ effect images), θ, provides a measure of the angular diameter distance of the cluster, $D_{\rm A} = L/\theta$. From the redshift of the cluster and $D_{\rm A}$ we can deduce the value of the Hubble constant.

This method is attractive since it works without any reference to the usual cosmological distance ladder, and an absolute measurement of the Hubble constant is made based on relatively simple physics (of the emission and scattering effects of hot gas held nearly in hydrostatic equilibrium in a cluster of galaxies). There are some drawbacks, of course. Most of these relate to the difficulty of determining the constant of proportionality in (6), which depends on the temperature of the cluster gas (measured by X-ray spectroscopy) and the detailed distribution of the gas within the cluster (usually modelled based on the X-ray image). Good models for the distributions of temperature and density may be difficult to obtain, since we measure only a projection of the cluster structure. In particular, we usually make the assumption that the cluster is spherical, isothermal, and has a density distribution described by a smooth model [2].

Nevertheless, the method has now been used to estimate the distances of nine clusters of galaxies: the results are displayed as a Hubble diagram in Fig. 7, and suggest a current best fit for a Hubble constant of 54 ± 8 (statistical) $\pm\, 10$ (systematic) $\rm km\,s^{-1}\,Mpc^{-1}$ [23].

Beware taking such an estimate at face value. The assumption of spherical symmetry for the clusters causes both an additional scatter and a systematic error. If clusters are non-spherical, then it is easiest to detect them in SZ effects and X-rays if they are oriented with their long axes on the line of sight. Thus we would expect a sample of clusters selected on surface brightness criteria to produce a Hubble constant estimate which is biased low, since the line-of-sight distance through the cluster estimated using (6) will be systematically high compared with the angular size. The extent of this bias is unknown, but it can be removed by producing a Hubble diagram based on a sample of clusters selected by total X-ray or SZ effect flux rather than surface brightness.

Small-scale clumping of the gas, undetected by the X-ray or SZ effect imaging, will also cause the Hubble diagram to be biased — this time to a Hubble constant which is systematically high. Sub-resolution clumping at some level is expected in all clusters: there are theoretical reasons to expect it not to be substantial, but this needs observational test through detailed X-ray spectroscopy.

It is easy to imagine other sources of systematic error: from thermal structure, contamination by the kinematic SZ effect or inverse-Compton X-ray emission, and so on. However, these effects should probably be small, and mostly will add to the scatter in the Hubble diagram (and so be lost in the errors of the individual distance measurements at present). More serious may be the difficulty imposed by the absolute nature of the distance estimate: to get the Hubble constant, we rely on the SZ effect and X-ray surface brightness that are measured being correct in absolute physical terms. However, this requires the SZ and X-ray instruments to be well calibrated — and it is not clear that this calibration is good at the level of 5 per cent or better. Indeed, since the distances in Fig. 7 are based on one X-ray telescope and only three radio telescopes, the number of truly independent Hubble constant measurements is less than the number of data-points on the diagram.

Baryon mass fraction

An interesting use of the SZ effect to measure the baryon mass fraction in a cluster was suggested by Myers et al. [24]. It is evident from (3) that the SZ effect depends on the projected electron density on the line of sight. For a known ionization state and gas metallicity, this means that the SZ effect is a direct measure of the mass of gas within the telescope beam. For some clusters, such as Abell 2218, we observe a bright population of arcs and a shear field evident in the weaker distortions of the shapes of background galaxies caused by gravitational lensing [25], as well as a strong SZ effect. Since the gravitational lensing is related to the cluster's total surface mass overdensity (and an image of the shear can be inverted to give a projected surface mass map), an SZ effect image can be directly divided by a mass map made from gravitational lensing data to produce a map of the ratio of baryonic to total mass as a function of position across the cluster.

Although this might be attempted by inverting an X-ray image to produce a map of the baryonic mass density, no such inversion is needed for the SZ effect data, and more reliable results should therefore result. This programme has not been successfully carried through for any cluster so far, although Myers et al. [24] were able to deduce overall baryonic mass fractions for three clusters in the range $(0.06-0.17)(H_0/100\ \mathrm{km\,s^{-1}\,Mpc^{-1}})^{-1}$ by using an estimate of cluster mass derived from galaxy dynamics rather than gravitational lensing.

Beware extending this result to the Universe as a whole: clusters may not be representative samples of the Universe, and it is likely that they show variations in the baryon to total mass ratio as a function of position. However, this is a very promising technique for studying the mass components of clusters and can be compared with the total mass distribution inferred from the X-ray image under the assumption of hydrostatic equilibrium to check the internal consistency of our understanding of cluster structures.

Cluster peculiar velocities

The spectrum of the combined (thermal plus kinematic) SZ effect near 218 GHz can be used to measure the peculiar (z-direction) velocity of a cluster relative to the Hubble flow. So far results have only been reported for two clusters, both at redshift ≈ 0.2 [17]. The apparent velocities were both consistent with zero, and imply that clusters move with velocities less than about 2000 $\mathrm{km\,s^{-1}}$.

Beware the effects of primordial anisotropy on such measurements, and also the requirement that the data have excellent relative calibration at all spectral bands used. This may be a particular problem when data are combined from several different telescopes with different angular resolutions.

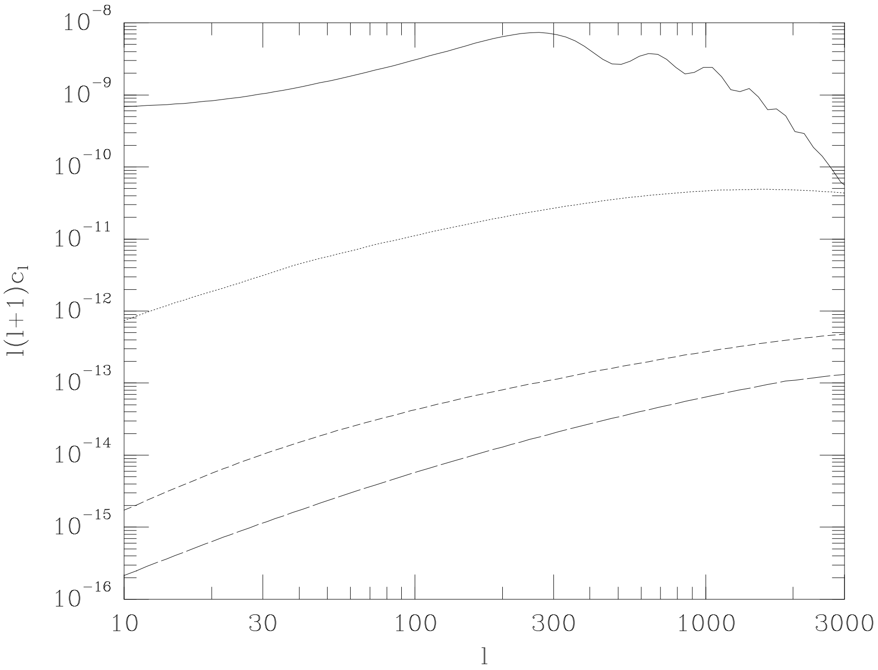

FIGURE 8. The zero-frequency power spectrum of primordial microwave background anisotropies (solid line), the thermal SZ effect (dotted line), the kinematic SZ effect (short dashed line), and the Rees-Sciama effect from moving clusters (long dashed line) predicted in the Λ-CDM cosmology discussed by Bahcall and Fan [30]. Figure from Molnar [9].

Confusion and cluster evolution

The SZ effect causes (small) changes in the integrated spectrum of the microwave background radiation and induces fluctuations in its brightness which appear superimposed on the fluctuations arising from the formation of structure in the early Universe. The angular scale of these SZ effect-derived structures depends on the manner in which clusters evolve and the large-scale structure of the Universe, and the redshift independence of SZ effects implies that a population of clusters with the same projected electron density and electron temperature, observed at different redshifts, will exhibit a minimum flux density (integrated over the cluster) at the redshift of maximum angular diameter distance in that cosmology [26]. In practice the use of SZ effect confusion to estimate cosmological parameters is complicated by the observational characteristics of the telescope used, the wide distribution in cluster properties, and the evolution of cluster atmospheres. Nevertheless the results of the OVRO RING experiment [27] have been used to show that an open Universe is unlikely if cluster atmospheres evolve only slowly with redshift [28].

When considered in the language of the power spectrum of fluctuations in the microwave background radiation, the relative weakness of SZ effect confusion on large angular scales, and the relative strength of the confusion on small angular scales, becomes apparent [9,29]. For $l \lesssim 3000$ the power spectrum tends to be dominated by the signal from primordial structures (Fig. 8), while the thermal SZ effect always dominates over the kinematic SZ and the Rees-Sciama effects of the clusters. The fact that we have so readily been able to measure SZ effects from individual clusters relies on those clusters being of relatively small angular size, and the association of their SZ effects with definite locations on the sky. However, the coming MAP and Planck satellites will be able to use the different spectral signatures of the thermal SZ effect and primordial anisotropies (only slightly affected by the kinematic SZ and Rees-Sciama effects) to measure the power spectra from the thermal SZ effect on scales $l \gtrsim 300$, providing a useful sample of detected clusters and information on cluster evolution (albeit over a relatively narrow range of angular scales).

Beware using the apparent SZ effect power spectrum to infer cosmological parameters, since this spectrum is heavily dependent on the (unknown) evolution of clusters. Even after the primordial fluctuation spectrum has been used to estimate the cosmological parameters, it will be difficult to invert the cluster power spectrum to deduce the history of cluster formation since the predicted spectrum is relatively featureless (Fig. 8).

PC 1643+4631

An interesting anomaly in the recent literature on SZ effects concerns the object PC 1643+4631 — a pair of QSOs for which Jones et al. [31] found a strong SZ effect (i.e., a reduction in the brightness of the microwave background radiation) despite there being no optical [32] or X-ray [33] evidence of a cluster of galaxies that might hold the gas needed to produce the SZ effect. The difficulty is that if the decreased brightness of the microwave background radiation is attributed to an SZ effect, then a massive cluster is needed at substantial redshift to hold the gas, but it is difficult to see how that cluster could have formed so early [34]. If the microwave background structure is interpreted in some other way, for example as a kinematic SZ effect from colliding QSO winds [35], a combined kinematic and thermal effect from an expanding hot gas bubble [36], or an extreme Rees-Sciama effect from mass motions, then even more extreme physical conditions are implied since the microwave background structure is so strong.

Beware: it is probably wrong to draw strong conclusions without a confirming measurement of the microwave background structure, preferably from a bolometric system which could provide some spectral information. This is a case where an improved map of the effect, with higher sensitivity and angular resolution, plus a deep X-ray image, would be of intense interest.

REFERENCES

1. Sunyaev, R.A. and Zel'dovich, Ya.B., Comm. Ap. Sp. Phys., 4, 173 (1974).
2. Birkinshaw, M., Phys. Rep. in press (1998).
3. Rephaeli, Y., ARAA, 33, 541 (1995).
4. Kompaneets, A.S., ZhEFT, 31, 876 (1956). Translation in Sov. Phys. JETP, 4, 730 (1957).
5. Fixsen, D.J. et al., 473, 576 (1996).
6. Rephaeli, Y., ApJ, 445, 33 (1995).
7. Itoh, N., Kohyama, Y. and Nozawa, S., ApJ, 502, 7 (1998).
8. Challinor, A. and Lasenby, A., ApJ, 499, 1 (1998).
9. Molnar, S.M., PhD Thesis, University of Bristol (1998).
10. Nozawa, S., Itoh, N. and Kohyama, Y., ApJ submitted (1998).
11. Sazonov, S.Y. and Sunyaev, R.A., ApJ in press (1998).
12. Phillips, P.R., ApJ, 455, 419 (1995).
13. Birkinshaw, M., Gull, S.F. and Northover, K.J.E., MNRAS, 197, 571 (1981).
14. Birkinshaw, M., Gull, S.F., Hardebeck, H.E. and Moffet, A.T., ApJ, submitted (1998).
15. Myers, S.T. et al., ApJ, 485,1 (1997).
16. Herbig, T., Lawrence, C.R., Readhead, A.C.S. and Gulkis, S., ApJ, 449, L5 (1995).
17. Holzapfel, W.L. et al., ApJ, 481, 35 (1987).
18. Blain, A.W., MNRAS, 297, 502 (1998).
19. Lamarre, J.-M. et al., ApJ, 507, 1 (1998).
20. Jones, M. et al., Nature, 365, 320 (1993).
21. Carlstrom, J.E., Joy, M. and Grego, L., ApJ, 456, L75 and ApJ, 461, L59 (1996).
22. Grainge, K., PhD thesis, University of Cambridge (1998).
23. Hughes, J.P., 'The Hot Universe', IAU Symp. 188, 189; eds Koyama, K., Kitamoto, S. and Itoh, M.; Kluwer Academic, Dordrecht (1998).
24. Myers, S.T. et al., ApJ, 485, 1 (1997).
25. Sarantini, D., Petrosian, V. and Lynds, R., ApJ, 458, 57 (1996).
26. Korolyov, V.A., Sunyaev, R.A. and Yakubtsev, L.V., Pis'ma Astr. Zh., 12, 339 (1986). Translation in Sov. Astr. Lett., 12, 141.
27. Myers, S.T., Readhead, A.C.S. and Lawrence, C.R., ApJ, 405, 8 (1993).
28. Markevitch, M. et al., ApJ, 426, 1 (1994).
29. Aghanim, N. et al., A&A, 334, 409 (1998).
30. Bahcall, N.A. and Fan, X., ApJ, 504, 1 (1998).
31. Jones, M.E. et al., ApJ, 479, L1 (1997).
32. Saunders, R.D.E. et al., ApJ, 479, L5 (1997).
33. Kneissl, R., Sunyaev, R.A., and White, S.D.M., MNRAS, 297, L29 (1998).
34. Bartlett, J.G., Blanchard, A. and Barbosa, D., A&A, 336, 425 (1998).
35. Natarayan, P. and Sigurdsson, S., MNRAS, in press (1998).
36. Aghanim, N. et al., A&A, 311, 1 (1996).